A Structural Theory for Non-stoicheiometry. Part II.† Defect Fluorite-type Structures: Lanthanoid Oxides MO_x with $1.50 \leqslant x \leqslant 1.72$

By **Bernard F. Hoskins and Raymond L. Martin,** Research School of Chemistry, Australian National University, P.O. Box 4, Canberra, A.C.T., Australia 2600

The hyperstoicheiometric composition region $MO_{1.500+\delta}$ of binary lanthanoid oxides is discussed in terms of the concept of octahedral oxygen co-ordination of anion vacant sites (c.d.s) in a fluorite-type (*C*1) lattice. The structural model proposed for the hypostoicheiometric composition range $MO_{2-\delta}$, based on isolated c.d.s, has been extended to the hyperstoicheiometric region by allowing for the formation of clustered defects, through their corner- and edge-sharing, achieved formally by the deletion of (213) oxygen-intact planes coupled with a crystallographic shear mechanism. The terminal member of the series *C*-M_2O_3 is shown to possess an anion lattice based on the tris-chelation of c.d.s with both chiral types being involved. Although ordered binary structures have not yet been found for the σ-region ($0 < \delta < 0.214$), this extension of the model seems to provide a useful insight into the phase characteristics of this grossly non-stoicheiometric region and, as well, affords a convenient description of the polymorphic transformation of the cubic type *C* to the hexagonal type *A* sesquioxides. The structure derived by this extension of the model for the M_6O_{10} phase is identical with that observed for the ternary oxides Sr_2UO_5 and Cd_2UO_5. The known structure of β-Bi_2O_3 is interpreted in terms of the corner-sharing of c.d.s in three dimensions. A structure for β-$Pr_{12}O_{22}$ is suggested on the basis of recently published unit-cell data.

(I) INTRODUCTION

THE binary system praseodymium oxide + oxygen has come to be regarded as a prototype for non-stoicheiometry derived from an ordered arrangement of anion vacancies on a superlattice of the fluorite-type (*C*1) parent structure.[1-9] At lower temperatures it has been established that the composition of intermediate ordered phases conform to a homologous series Pr_nO_{2n-2} ($n = 7$, 9, 10, 11, and 12). There is abundant evidence that the cation lattice remains intact in these MO_x (M = Ce, Pr, or Tb) phases so that variable stoicheiometry must be accommodated by an omission of oxygen atoms from $1/n$th of anion sites of the *C*1 lattice. In the absence of incisive *X*-ray, electron, or neutron diffraction structural information, the detailed nature and extent of ordering of anion vacancies at present remains unknown.[10]

In the previous paper,[11] the concept of an octahedrally co-ordinated anion vacancy $\square O_6$ was introduced in an attempt to devise a rational structural theory for the M_nO_{2n-2} series. The chemical composition of the resulting co-ordination defect (c.d.), $M_{7/2}\square O_6$, corresponds to that of the most stable homologue ι-$PrO_{1.714}$ (*i.e.* $n = 7$). This is the most reduced MO_x phase in which the c.d. can retain its structural integrity and independence. The arrangement of anion vacancies in the ι-phase is uniquely determined by the distinctive topology of the c.d., the vacant sites being gathered on oblique {213} planes which are separated by six oxygen-intact planes. The more closely-spaced vacancies lie in rows along $[\bar{1}\bar{1}1]$ and $\langle\bar{1}20\rangle$ consistent with strong short-range ordering forces between each vacancy and its six nearest oxygen neighbours. Since the overall composition of these planes is either $M\square_2$ or MO_2, the modular unit of $(n - 1)$ planes of MO_2 combined with one plane of $M\square_2$, characterizes a phase compositionally and yields the observed generic formula M_nO_{2n-2} for the more oxidized homologues. This extension of the model suggests that the anion deficiency in ordered MO_x phases in the hypostoicheiometric region ($1.714 \leqslant x \leqslant 2.000$) might likewise be accommodated by vacant sites gathered on oblique (213) planes interwoven with $(n - 1)$ oxide-intact planes.

Unfortunately, the number of possible structures which emerge from a topological analysis of the packing of c.d.s increases progressively for values of $n > 7$ and attention has been drawn [11] to some of the alternatives for $n = 8$ ($E8_1$ or pyrochlore structure), $n = 12$ (β and β′ $Pr_{12}O_{22}$ phases) and $n = 14$ ($Zr_{10}Sc_4O_{26}$ phase). Even though a unique solution of structure is not provided in these cases, the available evidence confirms that the co-ordination defect $M_{7/2}\square O_6$ is a fundamental structural unit which provides additional insight into the nature of these non-stoicheiometric oxides. Although no structure determinations have been published for Pr_nO_{2n-2} phases, a structure can be obtained for the β-$Pr_{12}O_{22}$, using the essentials of the above model, having unit-cell dimensions in exact agreement with those recently reported from *X*-ray and electron diffraction data.[10] This will be discussed further in Section IV.

Since the cation lattice remains essentially intact throughout the range $1.50 \leqslant x \leqslant 2.00$, ordering of the oxygen lattice presumably is achieved by co-operative jumps between oxygen anions and vacant sites; *viz.*:

$$O^{2-}/an + \square/an \rightleftharpoons \square/an + O^{2-}/an \qquad (1)$$

However, in order to undertake the topological analysis of Part I, it was found more convenient to consider the

† Part I is ref. 11.

[1] R. L. Martin, 'A Study of the Oxides of Praseodymium,' M.Sc. Thesis, University of Melbourne, 1948.
[2] R. L. Martin, *Nature*, 1950, **165**, 202.
[3] R. E. Ferguson, E. D. Guth, and L. Eyring, *J. Amer. Chem. Soc.*, 1954, **76**, 3890.
[4] A. F. Clifford and P. A. Faeth, Proc. 2nd Conf. Rare Earth Research, ed. J. F. Nachman and C. E. Lundin, Gordon and Breach, New York, 1962, p. 105.
[5] J. M. Honig, A. F. Clifford, and P. A. Faeth, *Inorg. Chem.*, 1963, **2**, 791.
[6] B. G. Hyde, D. J. M. Bevan, and L. Eyring, *Phil. Trans.*, 1966, **A259**, 583.
[7] J. Kordis, and L. Eyring, *J. Phys. Chem.*, 1968, **72**, 2044.
[8] T. C. Parks and D. J. M. Bevan, *Rev. Chim. Minérale*, 1973, **10**, 115.
[9] J. S. Anderson, ' Solid State Chemistry,' U.S. Nat. Bureau Standards Special Publication No. 364 (Washington), 1972, p. 295.
[10] L. Eyring and L. Tai, *Ann. Rev. Phys. Chem.*, 1973, **24**, 189.
[11] R. L. Martin, *J.C.S. Dalton*, 1974, 1335.

problem in terms of conceptual shearing of the *C*1 lattice and introducing y octants of composition $Pr_{1/2}O$ to the co-ordination defect $Pr_{7/2}\square O_6$ to generate the ordered phases of composition $Pr_{(7/2+1/2y)}\square O_{(6+y)}$. Shear vectors were defined which created a regular array of cavities in the ι-structure into which the additional $Pr_{1/2}O$ octants (of dimension $d = a/2$) could be incorporated whilst preserving the correct phasing of the cation sub-lattice and ensuring that the topological requirements of the c.d. are met. Crystallographic repeat units of the ensuing superstructures were then delineated on (001).

It will be apparent that the structures of the more reduced lanthanoid oxides in the hyperstoicheiometric region ($1{\cdot}500 \leqslant x \leqslant 1{\cdot}714$) can no longer be interpreted in terms of isolated $M_{7/2}\square O_6$ c.d.s. Negative values of y (−1, −2, and −3) give chemical compositions $M_3\square O_5$ ($x = 1{\cdot}667$), $M_{5/2}\square O_4$ ($x = 1{\cdot}600$), and $M_2\square O_3$ ($x = 1{\cdot}500$) but leave each anion vacancy co-ordinated by fewer than six non-bridging octants. However, octahedral co-ordination can, in principle, be restored if oxygen atoms are shared between contiguous pairs of vacant anion sites. Certainly, the known crystal structure of type-*C* ($D5_3$) lanthanoid sesquioxides [12-15] encourages the view that such an extension of the c.d. model should not only be valid but also provide a useful insight into the manner in which vacancies in the reduced oxides might conceivably be ordered.

Since the oxidized MO_x phases were previously [11] generated by the formalism of progressive incorporation of extra (213) planes of composition MO_2 into the type ι-M_7O_{12} lattice, we explore here the consequences of deleting successively single (213) planes of MO_2 from the ι-M_7O_{12} structure to obtain a description of reduced MO_x phases in the hyperstoicheiometric region. It will emerge that the structural relationships are better depicted on (010) rather than the (001) planes employed in Part I. Thus the previously described formation of an oxidized phase (*e.g.* for $y = 1$, ι-$Pr_7O_{12} \longrightarrow Pr_8O_{14}$) will be represented here in terms of a crystallographic shear along the trace of (213) on an (010) plane in the [$\bar{1}$01] direction. The procedure can most readily be visualized by employing the Anderson and Hyde 'scissor method' [16,17] whereby a drawing of an (010) structural layer or ι-M_7O_{12} is cut along the line along which oxygen sites are to be created and then opened up to effect the insertion (*i.e.* in such a way as to restore the tetrahedral co-ordination of the anions). For example, the production of an unoccupied (213) shear plane, characteristic of M_nO_{2n-2} is illustrated in Figure 1. Vacant oxygen and metal sites are created in equal numbers along [30$\bar{2}$] corresponding to $y = 1$, *i.e.* the formation of a (213) sheet of Pr_8O_{14} inserted coherently into the parent ι-Pr_7O_{12} matrix. The shear vector required to restore the cation lattice to the correct phase is $a/2$[$\bar{1}$01]. Since the new (213) plane is oblique, the additional oxygen and metal atoms do not lie on the same [30$\bar{2}$] line. Effectively, each new metal atom is displaced with respect to its oxygen counterpart by either $d/2$[$\bar{1}\bar{1}$1] or $d/2$[$\bar{1}$11] in an alternating sequence along [30$\bar{2}$]. The metal atom weight is one-half yielding the stoicheiometry MO_2 for the newly created (213) plane. The generation of the derived structure from its parent ι-M_7O_{12} may therefore be visualized as the insertion of one plane of MO_2 into a perfectly regular stack of six (213) planes of composition MO_2 and one of composition $M\square_2$ to yield the new phase $M_8\square_2O_{14}$ ($x = 1{\cdot}750$).

In this paper the procedure is inverted to consider possible structures of reduced MO_x phases which would result from the regular omission of (213) planes from the ι-M_7O_{12} parent by the shear mechanism. However, the properties and thermodynamic behaviour of the reduced lanthanoid oxides which require explanation will first be summarized.

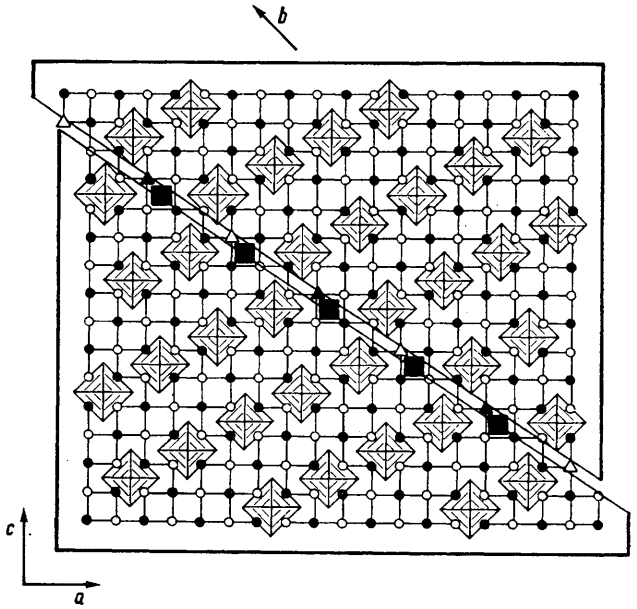

FIGURE 1 Formation of (213)$\frac{a}{2}$[$\bar{1}$01] shear plane, as in Pr_nO_{2n-2} ($n = 8$); b = Burgers vector (shear vector). ■; Δ; ▲ = inserted oxygen atoms at 0,0,0; metal atoms at $d/2$[$\bar{1}\bar{1}$1] and $d/2$[$\bar{1}$11], respectively

(II) PHASE RELATIONSHIPS IN REDUCED LANTHANOID OXIDES

The rhombohedral ι-M_7O_{12} phase is of central significance in the composition range $MO_{1.5}$—$MO_{2.0}$. Phases more oxidized than ι comprise the discrete homologues M_nO_{2n-2} at lower temperatures which are overlaid by the hypostoicheiometric f.c.c. α-phase at higher temperatures.[6] The α-phase is characterized by an extensive composition range and it occurs in lanthanoid and actinoid elements of variable oxidation state; *viz.* $CeO_{2-\delta}$, $PrO_{2-\delta}$, $UO_{2-\delta}$, $PuO_{2-\delta}$, $AmO_{2-\delta}$, $CmO_{2-\delta}$, and numerous ternary phases.[10] Evidence of

[12] L. Pauling and M. D. Schappell, *Z. Krist.*, 1930, **75**, 128.
[13] H. Dachs, *Z. Krist.*, 1956, **107**, 370.
[14] A. Fert, *Bull. Soc. Franc. Miner. Crist.*, 1962, **85**, 267.
[15] M. G. Paton and E. N. Naslen, *Acta Cryst.*, 1965, **19**, 307.
[16] J. S. Anderson and B. G. Hyde, *Bull. Soc. chim. France*, 1965, 1215.
[17] J. S. Anderson and B. G. Hyde, *J. Phys. and Chem. Solids*, 1967, **28**, 1393.

residual short-range order in this grossly non-stoicheiometric region has been alluded to elsewhere.[11,18] Unlike this oxygen-rich region, no ordered binary compounds have been observed [6-8] in the more reduced oxides in the hyperstoicheiometric region $MO_{1.5+\delta}$ with $(0 < \delta \lesssim 0.22)$. The terminal sesquioxides can crystallize in three different polymorphic forms (*A*-, *B*-, or *C*-type structures), the stable polymorph being determined both by its temperature of formation and the ionic radius of the lanthanoid.[19-25] At higher temperatures (*ca.* >800 °C) a grossly non-stoicheiometric b.c.c. $MO_{1.5+\delta}$ phase (designated σ) obtains. The maximum composition range varies with the nature of the lanthanoid and tends to narrow as the ionic radius of the tervalent cation is increased [26] being *ca.* $CeO_{1.67}$—$CeO_{1.72}$,[27-29] $PrO_{1.60}$—$PrO_{1.72}$,[6] and $TbO_{1.50}$—$TbO_{1.72}$ [7] for those lanthanoids which possess both +3 and +4 oxidation states.

A striking feature of the binary lanthanoid oxide + oxygen systems is the presence of a narrow miscibility gap between the b.c.c. σ-phase and the f.c.c. α-phase which persists to high temperatures.[6,28] For PrO_x this region is defined [6] by $1.695 \leqslant x \leqslant 1.725$. Similar regions of immiscibility between α and σ, of narrow compositional width, are also found for many ternary systems such as $(CeO_2 + Y_2O_3 + O_2)$.[1,30] It is significant that the unit-cell edge of binary oxides (expressed as the *C*1 dimension) varies linearly with composition (Vegard's Law) for the reduced σ-phases, whereas positive deviations frequently occur for the more oxidized α-region. This pattern of behaviour is reproduced in many ternary lanthanoid oxide + oxygen systems and points to a fundamental structural difference between the σ- and α-phases.

The phase relationships in the hyperstoicheiometric $MO_{1.5+\delta}$ region have been exhaustively explored for praseodymium [6,7] and terbium [7,31] but are less well characterized for cerium because the oxygen dissociation pressures above CeO_x are many orders of magnitude lower.[26-29] The praseodymium oxide + oxygen system exhibits the most varied tensimetric behaviour, and accordingly best illustrates the phase phenomena which must be accommodated by any structural model.

The detailed phase diagram of the $PrO_x + O_2$ system [6-8] shows that the σ-phase possesses a eutectoid at 910 °C. Above this temperature ι-$PrO_{1.714}$ is reduced to the non-stoicheiometric σ-phase whose range of composition (*cf.* Table) is determined by oxygen

TABLE

Composition of hyperstoicheiometric σ-PrO_x [6]

P_{O_2}/Torr	x in σ-PrO_x (t/°C)
10	1·65 (930)—1·60 (1068)
45	1·67 (975)—1·60 (1070)
205	1·675 (1020)—1·645 (1130)
650	1·695 (1065)—1·67 (1130)

pressure (and necessarily temperature). Reduction of σ- to θ-$PrO_{1.500}$ (*i.e.* type *A*) is observed at oxygen pressures below *ca.* 10 Torr. $PrO_{1.500}$ Is reoxidized directly to ι-$PrO_{1.714}$ without the intervention of a σ precursor at an oxygen pressure of *ca.* 5 Torr. At higher pressures (*e.g.* >10 Torr), $PrO_{1.500}$ reoxidizes to ι-$PrO_{1.714}$ *via* the σ-phase.

Below 910 °C there is evidence that both the σ-and ι-phases exist in reduction as metastable forms σ^m and ι^m at low oxygen pressures. Thus reduction of ι-$PrO_{1.714}$ below 910 °C results in the reversible equilibrium $\iota^m \rightleftharpoons \sigma^m$ where σ^m inhabits the composition range *ca.* $1.60 \leqslant x \leqslant 1.64$ in the range 1.6—10^{-3} Torr. Further reduction results in the irreversible conversion $\sigma^m \longrightarrow$ θ-$PrO_{1.5}$ and there is evidence of coherent intergrowth between this θ and σ^m upon subsequent reoxidation or reduction. Although $\sigma^m \longrightarrow$ θ-$PrO_{1.5}$ at higher temperatures, it also appears to be continuous with φ-$PrO_{1.5}$ (*i.e.* type *C*) when reduced at lower temperatures.[8]

Isobaric heating and cooling cycles for $PrO_x + O_2$ are characterized by substantial hysteresis in this hyperstoicheiometric composition region which points to structural similarities between the reactant and product phases involved and leads to the expectation of coherent intergrowth between them.[32] The term *pseudo-phase* has been introduced by Hyde and Eyring [6,31] to describe those reactions which are bivariant in one direction (say, oxidation), but monovariant when reversed (say, reduction). Coherence between structurally similar reactant and product promotes epitaxial continuity between them to yield intergrown domains which, although diphasic, actually exhibit reproducible bivariant apparently ' monophasic ' behaviour.

Detailed structural characterization of pseudo-phases remains unresolved. For example, in the $PrO_x + O_2$ system, high-temperature diffraction studies of the (αι) and (σι) pseudo-phases confirm that they are diphasic over their entire existence range.[33,34] It has been

[18] M. S. Jenkins, R. P. Turcotte, and L. Eyring, ' Chemistry of Extended Defects in Non-Metallic Solids,' ed. L. Eyring and M. O'Keefe, North Holland Co., Amsterdam, 1970, p. 36.

[19] R. S. Roth and S. J. Schneider, *J. Res. Nat. Bur. Stand.*, 1960, **A64**, 309.

[20] I. Warshaw and R. Roy, *J. Phys. Chem.*, 1961, **65**, 2048.

[21] J. C. Wallmann, *J. Inorg. Nuclear Chem.*, 1964, **26**, 2053.

[22] D. S. Chapin, M. C. Finn, and J. M. Honig, ' Rare Earth Research III,' ed. L. Eyring, Gordon and Breach, New York, 1965, p. 607.

[23] H. Hoekstra, *Inorg. Chem.*, 1966, **5**, 754.

[24] M. Foex and J-P. Traverse, *Compt. rend.*, 1966, **262**, 636.

[25] T. D. Chikalla and R. P. Turcotte, Proc. 5th Materials Research Symposium, Nat. Bureau Standards Special Publ. No 364, 1972, p. 319.

[26] T. C. Parks and D. J. M. Bevan, *Rev. Chim. Minérale*, 1973, **10**, 15.

[27] D. J. M. Bevan, *J. Inorg. Nuclear Chem.*, 1955, **1**, 49.

[28] D. J. M. Bevan and J. Kordis, *J. Inorg. Nuclear Chem.*, 1964, **26**, 1509.

[29] Y. Ban and A. S. Nowick, ' Solid State Chemistry,' U.S. Nat. Bureau Standards Special Publication No. 364, Washington, 1972, p. 353.

[30] D. J. M. Bevan, W. W. Barker, R. L. Martin, and T. C. Parks, ' Rare Earth Research,' ed. L. Eyring, Gordon and Breach, New York, 1965, **3**, 441.

[31] B. G. Hyde and L. Eyring, ' Rare Earth Research,' ed. L. Eyring, Gordon and Breach, New York, 1965, **3**, 623.

[32] L. Eyring, *J. Solid State Chem.*, 1970, **1**, 376.

[33] D. A. Burnham and L. Eyring, *J. Phys. Chem.*, 1968, **72**, 4415.

[34] D. A. Burnham, L. Eyring, and J. Kordis, *J. Phys. Chem.*, 1968, **72**, 4424.

pointed out [33] that randomly oriented domains of the order of 5—20 unit cells in extent with linear dimensions of *ca.* 25—100 Å should yield broad diffraction lines with poor resolution in the hysteresis regions. In fact, quite sharp reflections are generally found for both the reactant and product components of the pseudo-phases which requires that assemblies of microdomains must be arranged in phase to yield coherently diffracting regions of at least 500 Å in their linear dimension.

Extensive tensimetric studies of the related binary (terbium–oxygen) [31,35] and the ternary (praseodymium–terbium–oxygen) [7] and (terbium–cerium–oxygen) [35] systems provide additional evidence for pseudo-phase formation in the hysteresis loops of the two-phase regions. Although the observed *p–t–x* behaviour is non-classical, it is reproducible in these regions and is consistent with the formation of domains of ι-phase coherently intergrown with adjoining phases such as σ and α.

In summary, the predominant features of the hyperstoicheiometric $MO_{1\cdot5+\delta}$ region which require explanation are as follows: (i) the absence of ordered line phases; (ii) the origin of the gross non-stoicheiometry exhibited by the σ-phase and the temperature dependence of its phase boundary; (iii) the existence of the (σι) pseudo-phase; (iv) the existence of metastable σ^m and ι^m regions; (v) the nature of the immiscibility gap between σ- and α-phases; and (vi) the transformation of cubic type *C* to hexagonal type *A*-M_2O_3 (or monoclinic type *B*-M_2O_3).

(III) STRUCTURAL MODELS FOR THE HYPERSTOICHEIOMETRIC REGION $MO_{1\cdot5+\delta}$

σ_1 *Region* ($1\cdot692 \geqslant x \geqslant 1\cdot667$).—For M = Pr, ordered phases have been characterized for the members $n = 4$, 7, 9, 10, 11, and 12 in the homologous series M_nO_{2n-2}. If $n = 6$, the composition M_6O_{10} (*i.e.* $MO_{1\cdot667}$) is obtained. It is proposed here that the formation of this phase from the known ι-M_7O_{12} structure can be formally described in terms of the systematic deletion of one-sixth of the (213) planes of composition $M_{1/2}O$ accompanied by an appropriate crystallographic shear operation to restore the metal lattice to the correct phase. A formal mechanism for the production of a shear plane in ι-M_7O_{12} is illustrated in Figure 2. A characteristic (010) plane of the parent ι-phase which passes through oxygen and vacancy sites is shown in Figure 2 (a). In this plane, the c.d.s lie on rows in the [30$\bar{2}$] direction which are the lines of intersection of the (213) planes of composition $M_{1/2}\square$ with the (010) plane in question. Between adjacent [30$\bar{2}$] rows of c.d.s there are six rows of oxygen atoms related to the (213) planes of composition $M_{1/2}O$ to yield the overall composition for the ι-phase of $M_{7/2}\square O_6$. If the [30$\bar{2}$] line of oxygen atoms indicated in Figure 2 (a) is removed, together with the associated metal atoms which lie along the parallel dashed lines, this corresponds to the removal of a single (213) plane of composition $M_{1/2}O$ in the three-dimensional structure.

[35] J. Kordis and L. Eyring, *J. Phys. Chem.*, 1968, **72**, 2030.

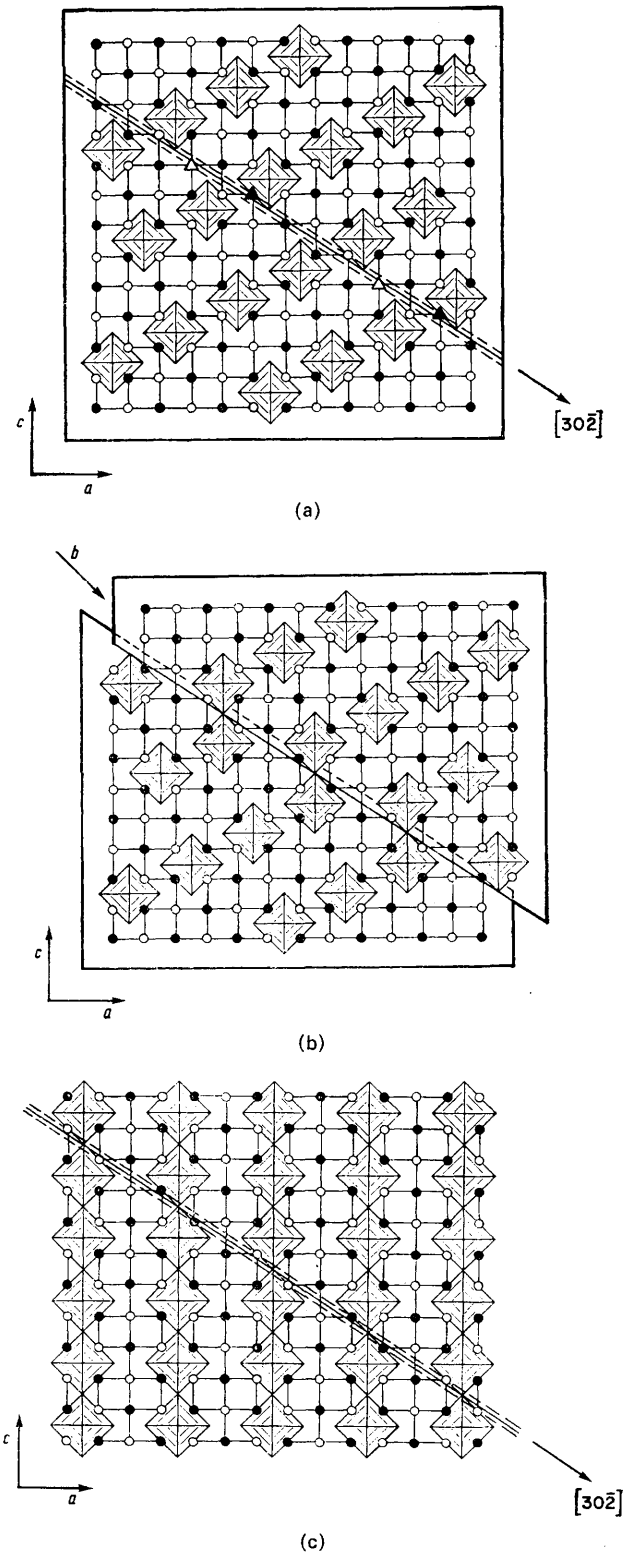

FIGURE 2 (a) Idealized (010) layer of ι-Pr_7O_{12} showing the [30$\bar{2}$] lines on which oxygen (full line) and Pr atoms (dashed lines and indicated by △ and ▲) are to be eliminated. (b) Formation of corner-shared c.d.s in $(213)^a_2[\bar{1}01]$ shear plane; *b* = Burgers vector. (c) Conjectural structure for $MO_{1\cdot667}$ phase ($n = 6$) based on infinite rows of corner-sharing c.d.s along [001]. The lines of Pr and O atoms to be eliminated to form a [30$\bar{2}$] row of edge-shared c.d.s are also shown (*cf.* Figure 3)

If the elimination is accompanied by a crystallographic shear $a/2[10\bar{1}]$, the $C1$ metal lattice is restored and a row of paired corner-sharing c.d.s is generated along the $[30\bar{2}]$ direction as shown in Figure 2 (b). The composition of each discrete pair is $M_{13/2}\square_2O_{11}$ or $MO_{1\cdot692}$. The systematic elimination of one-sixth of all (213) planes of composition $M_{1/2}O$ results in a structure of composition $M_6\square_2O_{10}$ or $MO_{1\cdot667}$ with infinite rows of corner-sharing c.d.s in the [001] direction as depicted in Figure 2 (c). It will be apparent that space-filling structures based on discrete rather than infinite clusters, each comprised of $(m+1)$ linear corner-sharing c.d.s can be derived from the ι-phase by the regular omission of $\left(\frac{m}{m+1}\right)1/6$ of the oxygen-containing (213) planes. The composition of these clusters lies in the range $1\cdot692 > x > 1\cdot667$ and is given by $M_{(3m+3\cdot5)}\square_{(m+1)}O_{(5m+6)}$. For example, if $m = 1$, one-twelfth of the oxygen-intact (213) planes are systematically deleted to generate a structure based on close-packed discrete pairs of corner-sharing c.d.s to yield an ordered phase of composition $MO_{1\cdot692}$. The value $m = 0$ corresponds to the isolated c.d. or ι-phase while $m = \infty$ gives the terminal $MO_{1\cdot667}$ phase illustrated in Figure 2 (c).

The topology of the corner-sharing clusters determines that the anion vacancies remain gathered on $(m+1)$ sets of (213) planes, the $(m+1)$ sets occurring at regularly-spaced intervals throughout the structure.

Since reduction of the relatively stable ι-phase occurs at higher temperatures, it might be anticipated that the formation of discrete ordered phases is unlikely. Rather the sequence of (213) planes of vacancies is likely to be irregular corresponding to clusters of variable chain length. In this event a continuum of coherently intergrown phases of remarkably similar structural characteristics would form the basis of the grossly non-stoicheiometric σ-phase MO_x in the composition region $1\cdot692 > x > 1\cdot667$.

σ_2 *Region* ($1\cdot667 \geqslant x \geqslant 1\cdot600$).—For $n = 5$, the composition M_5O_8 (*i.e.* $MO_{1\cdot600}$) is obtained. In an analogous way to the above, the systematic removal of one-fifth of the (213) oxygen-intact planes from the M_6O_{10} structure accompanied by a $a/2[10\bar{1}]$ crystallographic shear yields a structure of composition M_5O_8. This is based on rows of edge-sharing c.d.s along the [101] direction and the characteristic f.c.c. metal lattice. One of the $[30\bar{2}]$ lines along which oxygen and metal atoms are removed is shown in Figure 2 (c) and the derived M_5O_8 structure is illustrated in Figure 3.

Alternatively, the M_5O_8 can be derived directly from the ι-phase by the removal of two (213) oxygen-intact planes followed by a crystallographic shear of $a[10\bar{1}]$ to give the structure in Figure 3. Again, close-packed structures can be envisaged based on discrete rather than infinite edge-sharing c.d. clusters. The regular omission of $\left(\frac{m}{m+1}\right)2/6$ of the (213) planes gives clusters of composition $M_{(2\cdot5m+3\cdot5)}\square_{(m+1)}O_{(4m+6)}$ in the range $1\cdot667$ $(m = 1) \geqslant x \geqslant 1\cdot600$ $(m = \infty)$. The topology of the linear clusters of complexity $(m+1)$ permits close packing with the retention of the f.c.c. metal lattice.

The lack of definition observed in this region of the phase diagram is not surprising since fragmentation by oxidation of the M_5O_8 linear infinite chains into discrete clusters of shorter chain length can be expected. Again, a continuum of coherent intergrowths would extend the non-stoicheiometric σ-phase into the composition region $1\cdot667 \geqslant x \geqslant 1\cdot600$.

σ_3 *Region* ($1\cdot600 \geqslant x \geqslant 1\cdot500$).—For $n = 4$ the terminal sesquioxide composition M_4O_6 (*i.e.* $MO_{1\cdot500}$) is obtained. The removal of one-quarter of the (213) $M_{1/2}O$ planes from the M_5O_8 precursor accompanied by the $a/2[10\bar{1}]$ crystallographic shear yields a structure of composition $MO_{1\cdot500}$ based on a combination of corner- and edge-sharing c.d.s in the [100] and [011] directions, respectively. The structure of a single (010) layer illustrated in Figure 4 (a) reveals only the

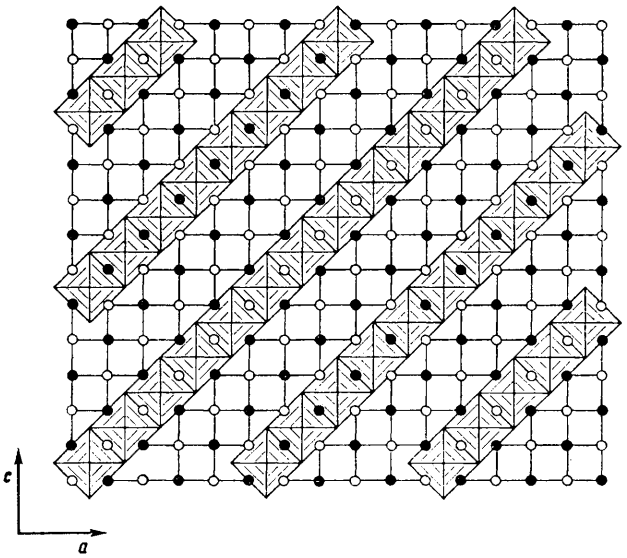

FIGURE 3 Conjectural structure for $MO_{1\cdot600}$ phase ($n = 5$) based on infinite rows of edge-sharing c.d.s along [101]

corner-sharing of c.d.s. The associated concomitant edge-sharing which occurs between adjacent [100] lines of corner-sharing c.d.s is shown in Figure 4 (b). For convenience, we will refer here to this sesquioxide structure as type *D*.

Again, this M_4O_6 structure can be regarded as a derivative of the ι-phase formed by the removal in a regular fashion of three (213) $M_{1/2}O$ planes accompanied by the crystallographic shear of $3a/2[10\bar{1}]$ so that the close-packed structure involving corner- and edge-sharing shown in Figure 4 is obtained. Since an infinite sharing of c.d.s in three- rather than two-dimensions is now involved, it seems to us that structures based on smaller discrete clusters will be less common in this region. The omission of $\left(\frac{m}{m+1}\right)2/6$ of contiguous planes, together with $\left(\frac{l}{l+1}\right)1/6$ of the (213) planes, will lead to edge- and corner-sharing clusters

conforming to the composition $M_{(2\cdot5m+3l+3\cdot5)}\square_{(m+l+1)}O_{(4m+5l+6)}$. The available tensiometric and isobaric studies confirm that the non-stoicheiometric σ-phase terminates at the composition $x = 1\cdot600$ for M = Pr

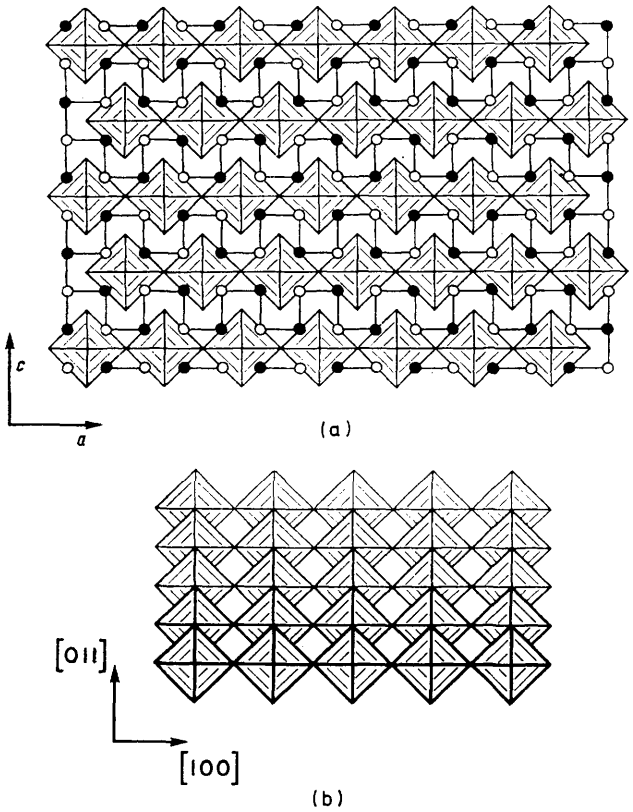

FIGURE 4 Structure of type D-$MO_{1\cdot500}$ phase ($n = 4$) based on a combination of corner- and edge-sharing c.d.s. (a) Corner-sharing of c.d.s along [100]. (b) Edge-sharing of c.d.s along [011] (The metal atoms have not been included.)

and there is no evidence for other phases between this and the sesquioxide. However, this is not the case for M = Tb for which the σ-phase extends from $TbO_{1\cdot714}$ to $TbO_{1\cdot500}$.

We have attempted to rationalize the σ-region in terms of the elimination of oxygen-intact planes of the ι-phase parallel to vacancy-only planes in orientations other than (213). It emerges that for other planes such as (1$\bar{3}$5) the anion sub-lattice can only be restored by a shear vector $a/2$[100] which places anions and vacancies in octants of the $C1$ structure of opposite metal orientation. Under these conditions, the metal lattice can no longer be regarded as being invariant to crystallographic shear.

Polymorphic Relationships of the M_2O_3 *Sesquioxides.*—Metal sesquioxides with the type D structure have not been reported and the known arrangements of the lanthanoid(III) oxides have been designated $A(\theta;\ D5_2)$,[36,37] B,[38] and $C(\phi,\ D5_3)$.[12-15]

The type C-M_2O_3 is closely related to the $C1$ fluorite MO_2 structure. It involves a regular omission of one-quarter of the oxygen atoms, a small distortion of the metal lattice from f.c.c., and a unit cell of b.c.c. symmetry with double the fluorite cell edge. For the present discussion the structure can be idealized to f.c.c. without the loss of any significant features.

It is particularly striking that every vacant anion site in C-M_2O_3 is co-ordinated by an octahedron of near oxygen neighbours to yield an anion lattice based on

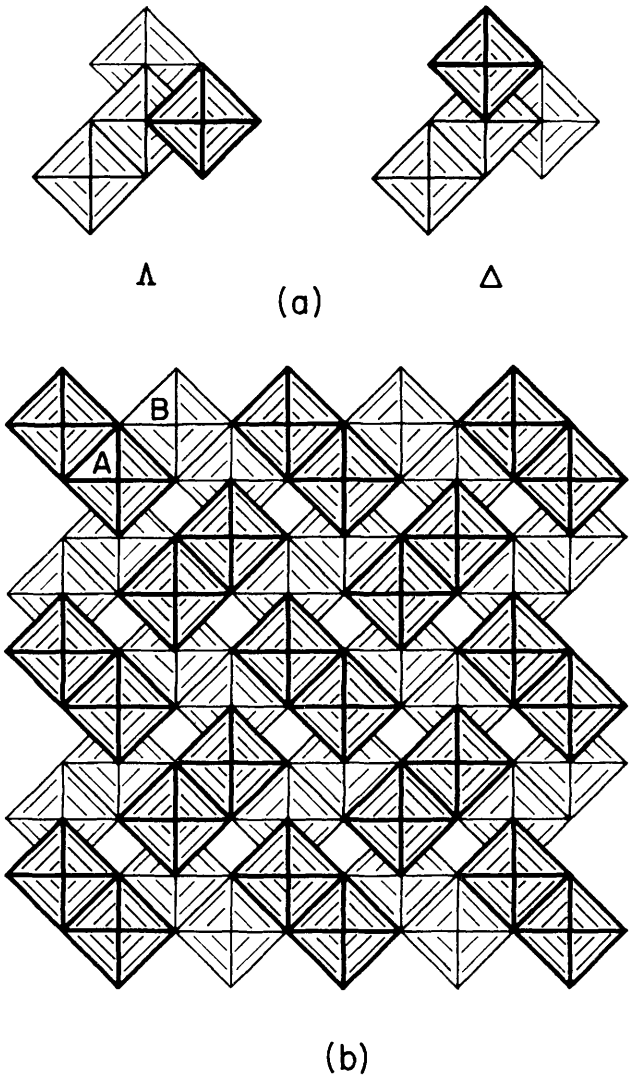

FIGURE 5 Structure of type C lanthanoid sesquioxides ($D5_3$). (a) Clusters of four edge-sharing c.d.s showing central c.d. with opposite chiralities (Λ and Δ). (b) Two adjacent {100} layers of the type C-M_2O_3 lattice. (Metal atoms have not been included.) The c.d.s designated A and B represent a typical pair from adjacent {100} layers which lie on one of the four non-intersecting ⟨111⟩ directions

c.d.s. We have already drawn attention to the structure-determining role of this entity in other oxides such as the M_7O_{12} and pyrochlore ($E8_1$) M_8O_{14} phases.[11] In the three-dimensional array of c.d.s of C-M_2O_3 each $\square O_6$-octahedron shares three edges with three $\square O_6$ nearest-neighbours. These, and hence the edges involved, are related by a three-fold symmetry axis passing through

[36] L. Pauling, *Z. Krist.*, 1929, **69**, 415.
[37] W. C. Koehler and E. O. Wollan, *Acta Cryst.*, 1953, **6**, 741.
[38] D. T. Cromer, *J. Phys. Chem.*, 1957, **61**, 753.

the centrally co-ordinated c.d. and all four c.d.s are situated on the same {111} plane. A fragment of the structure showing a cluster of four edge-sharing c.d.s viewed down one of the cubic crystallographic axes is sketched in Figure 5 (a).

Two adjacent layers parallel to {100} of the cubic C-M_2O_3 structure are illustrated in Figure 5 (b).

This representation of the type-C structure based on edge-sharing of c.d.s can be related to the more usual description, as containing non-intersecting strings of oxygen vacancies along all four ⟨111⟩ directions, in the following way. In Figure 5 (b) we have designated, by the letters A and B, a typical pair of c.d.s from adjacent {100} layers, which lie on one of these ⟨111⟩ directions. The identification of similarly related pairs defines the remaining ⟨111⟩ directions. It is interesting to note that the c.d.s A and B are of differing chiral types.

The edge-sharing between c.d.s within each {100} layer of the type-C structure produces a distinctive pattern of isolated 'pairs' which differs from the chains of corner- and edge-sharing c.d.s which characterize the type-D structure [Figure 6 (a) and (b)]. However, there is, in fact, a close relationship between the two which can be formally represented in the following manner. Consider the (100) layer of D-M_2O_3 shown in Figure 6 (a): if we divide the edge-sharing chains into pairs and rotate each alternate pair by $\pi/2$ radians, we arrive at the arrangement of anion vacancies which characterizes the type-C structure as shown in Figure 6 (c). This rotation occurs co-operatively in all layers throughout the lattice. It will be apparent that each rotation operation on a pair of edge-sharing c.d.s is equivalent to the co-operative exchange between the two oxygen anions forming the shared edge with their co-ordinated vacancies [*cf.* equation (1)]. This is also shown in Figure 6 (a).

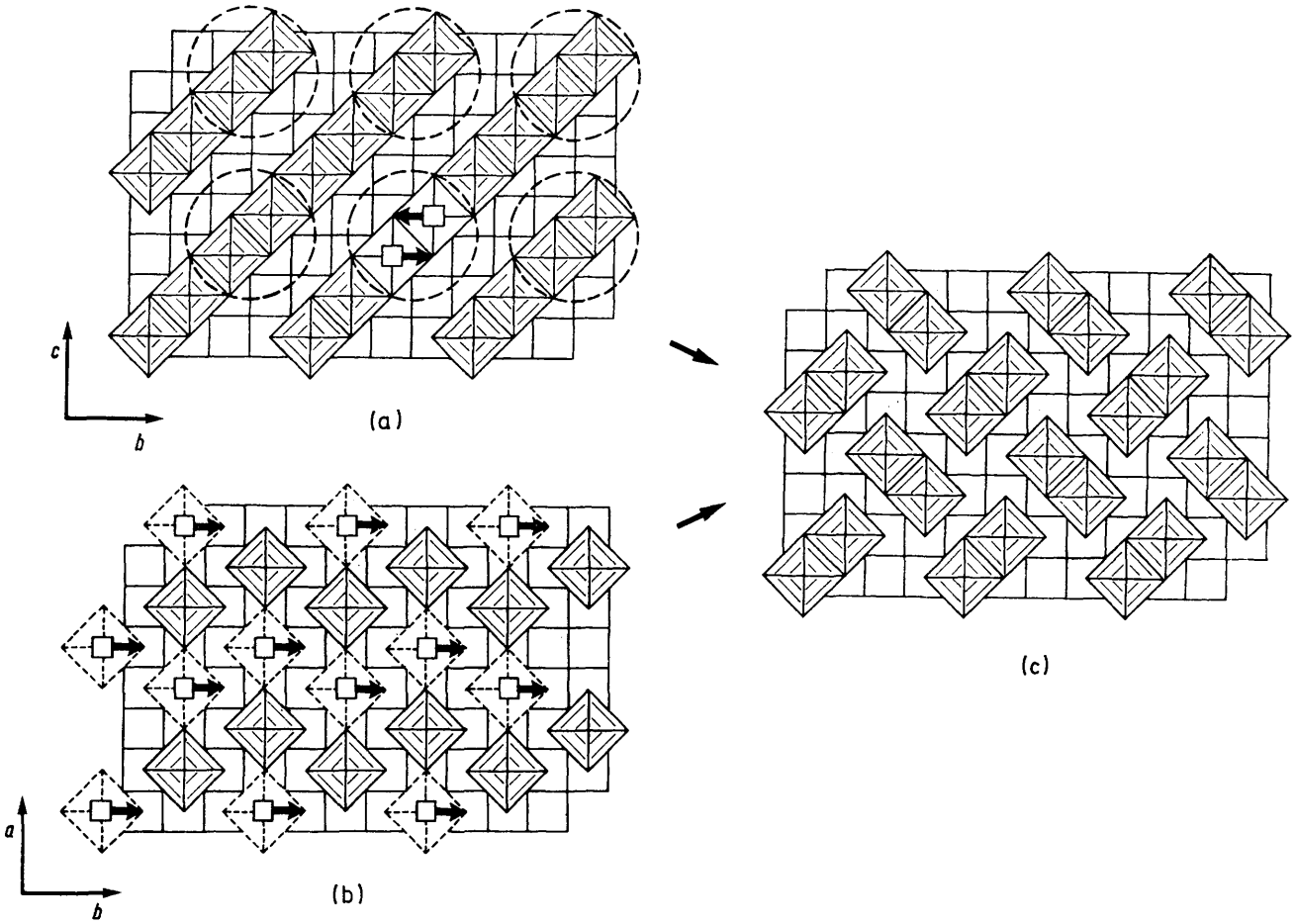

FIGURE 6 Transformation of type $D \longrightarrow$ type C-M_2O_3. (a) (100) layer of type D structure illustrating how a concerted oxygen $\rightleftharpoons$ vacancy switch is equivalent to a rotation through $\pi/2$ radians of an edge-sharing pair of c.d.s. (b) An (001) layer of type D-M_2O_3 showing a series of concerted oxygen $\rightleftharpoons$ vacancy switches for the type D to C transformation. (c) {100} Layer of the cubic-type C structure derived from type D by the mechanisms depicted in (a) and (b)

Alternatively, the process can be depicted in an (001) layer by the series of concerted oxygen-vacancy switches as shown in Figure 6 (b). This model for type-D to -C transformation only requires an oxygen-vacancy exchange over the minimum possible distance.

For the early lanthanoid elements, it is found that the type C-M_2O_3 is stable at lower temperatures but transforms irreversibly at higher temperatures to either the hexagonal type A or monoclinic type B modific-

ations.[19-25] Both these structures can be depicted using the matrix representation based on octants of the fluorite cube since their oxygen lattice remains complete. In the true crystallographic A and B structures there are considerable distortions of the O_8-cubes with the metal atoms being displaced from their cube centres. However, when the structures are idealized, the atomic displacements of the oxygen and metal lattices which differentiate them disappear so that for the present purposes types A and B are equivalent. This can be seen readily if the A and B structures are viewed in their $[211]_A$ and $[001]_B$ directions which correspond to a $\langle 100\rangle_{cub}$ direction in each of the idealized structures.

We will now consider a plausible mechanism whereby the type D structure can be transformed into the high-temperature hexagonal type A modification. It is seen from Figure 7 (a) that in any (100) layer, the anion vacancies lie in rows along [011]. This constitutes the line of intersection of this (100) layer with an oblique $(2\bar{1}1)$ plane on which the c.d.s are gathered. If the [011] rows of vacancies are annihilated by a c.s.

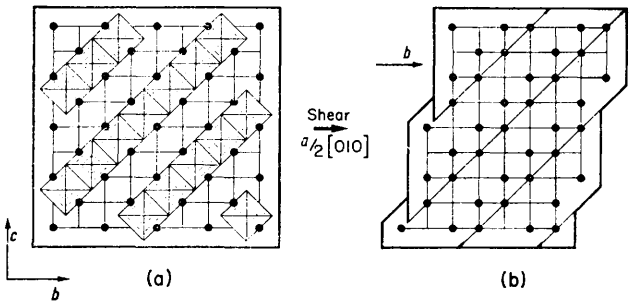

FIGURE 7 Transformation of type $D \longrightarrow$ type A-M_2O_3. (a) Rows of vacant anion sites along [011] in type D structure with f.c.c. metal atom lattice. (b) Annihilation of anion vacancies by shear vector $\frac{a}{2}[010]$ to give h.c.p. metal of type A ($D5_2$) sesquioxides

$a/2[010]$ * to form a completed oxygen lattice, then for this plane the f.c.c. metal lattice is transformed concomitantly to that which characterizes the idealized types A and B sesquioxide; this is shown in Figure 7 (b). This procedure conforms to the formal structural relationships between CaF_2 and La_2O_3 discussed by Hyde.[39]

Anderson and Hyde have proposed [17] a plausible dislocation mechanism for producing the homologous Magnéli phases from the ReO_3 and TiO_2 parents. In reduction it is suggested that an aggregation of anion vacancies into a disc occurs across which the lattice collapses followed by the c.s. operation. The vacant sites are thereby eliminated and the original cation co-ordination is restored.

In order to apply this mechanism to the transformation of either type C or D into type A, the anion vacancies must be gathered on to $\{111\}_{cub}$ planes as the necessary precursor to collapse and c.s. of the f.c.c. lattice. In the type D structure, the vacancies are gathered on $(\bar{2}\bar{1}1)$ [as well as $(2\bar{1}1)$ and (213)] planes. It is easy to envisage the transposition of all vacancies on to $(\bar{1}\bar{1}1)_{cub}$ for this structure by single oxygen-vacancy site switches for those vacancies not already residing on these planes in the manner shown for a (010) layer in Figure 8.

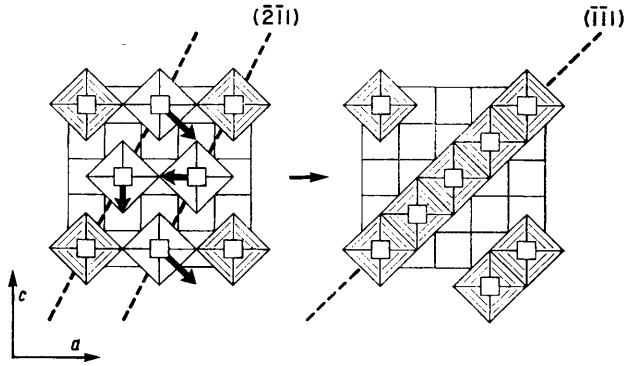

FIGURE 8 Transposition of vacant anion sites from $(\bar{2}\bar{1}1)$ planes of type D-M_2O_3 to $(\bar{1}\bar{1}1)$ planes by oxygen $\rightleftharpoons$ vacancy site switches

Before proceeding, it is instructive to reconsider the structure of type C-M_2O_3 in terms of its sequence of {111} anion planes. Relative to $C1$-MO_2 every {111} layer of oxygen atoms has one-quarter of the oxygen positions vacant to yield the stoicheiometry M_2O_3. The anion vacancies are organized so that each is octahedrally co-ordinated by oxygen to preserve the $\square O_6$ entity. The arrangement of vacancies on a (111) plane is illustrated in Figure 9 which reveals that they are gathered in groups of four comprised of edged-sharing c.d.s. These can be identified with the Y-shaped group of anion vacancies of three-fold symmetry commented on by Eyring and Holmberg.[40] Furthermore, the

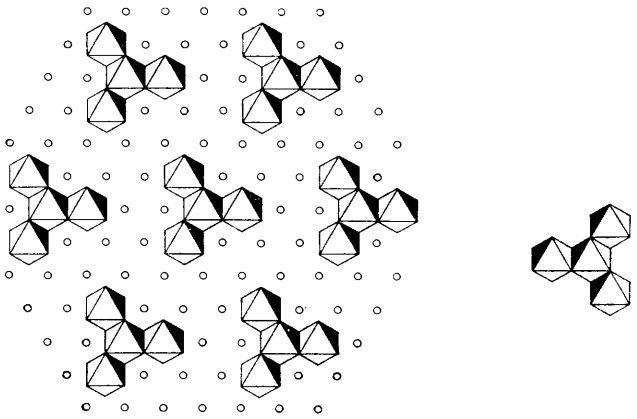

FIGURE 9 Arrangement of vacant anion sites on a (111) plane of type C-M_2O_3 showing their co-ordination polyhedra. The Λ chirality of the Y-shaped clusters in this plane is contrasted with the Δ configuration of adjoining (111) planes shown in the inset

arrangement of vacancy clusters with respect to each other is such as to preserve the three-fold symmetry.

Each c.d. is tris-chelated by its three neighbouring

* c.s. = Crystallographic shear.

[39] B. G. Hyde, *Acta Cryst.*, 1971, **A27**, 617.

[40] L. Eyring and B. Holmberg, *Adv. Chem. Ser.*, 1963, **39**, 46.

c.d.s, conferring on it the property of chirality, *i.e.* Δ and Λ configurations occurring equally. In particular, it will be observed that in any (111) layer only one particular chiral type occurs. However, adjacent (111) layers involve Y-shaped clusters of opposite chirality.

The property of chirality determines the manner in which Y-shaped clusters link with their neighbours in the high temperatures involved. If the $C1$-MO_2 structure is viewed in terms of its sequence of {111} atomic planes, the *A*, *B*, *C*, *etc.* of {111} oxygen and metal atom planes can be represented as that shown in Figure 12 (a). By gathering the anion vacancies of the idealised C-M_2O_3 structure on to every fourth {111} anion plane, the sequence is as shown in Figure 12 (b).

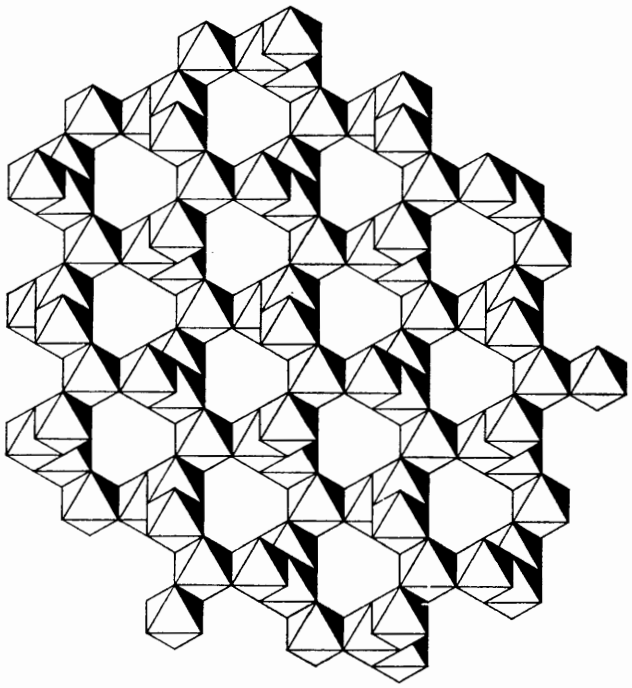

FIGURE 10 One of the two interpenetrating networks of c.d.s (Λ chirality) showing the edge-sharing involved between layers 1, 3, and 5

next-nearest, rather than nearest, layers. Two interpenetrating but unconnected networks of c.d.s, each of opposite chirality, are thereby generated throughout the C-M_2O_3 structure, one involving the layers numbered 1, 3, 5, *etc.* and the other 2, 4, 6, *etc.* The edge-sharing involved between layers 1, 3, and 5 is shown in projection on $(111)_{cub}$ in Figure 10.

Layer 7 exactly overlays layer 1 of this diagram and this pattern repeats itself throughout the lattice. The projection of the even-numbered layers, *i.e.* those of opposite chirality, overlaps such that the lacunae of the projection shown in Figure 10 are removed.

Whereas Anderson and Hyde's proposal involves the elimination of planes of oxygen to give reduced Magnéli oxides, we apply it here to the polymorphic transformation of cubic type *C* to hexagonal type *A* sesquioxides. The first step in the high-temperature transformation is the rearrangement of four adjacent {111} anion planes, each containing one-quarter vacancies, to three adjacent oxygen-intact planes with the fourth containing only vacancies as is illustrated in Figure 11. The distance required for oxygen $\rightleftharpoons$ vacancy switches to achieve this are 50% through *d*, *i.e.* along the edge of an octant, and 25% through $d\sqrt{2}$, *i.e.* across the face of an octant. These displacements are relatively small considering

The composition of a single {111} layer of c.d.s is $M_{3/2}\square O_2$. This group may be discerned in Figure 12 (b) together with an associated {111} plane of oxygen

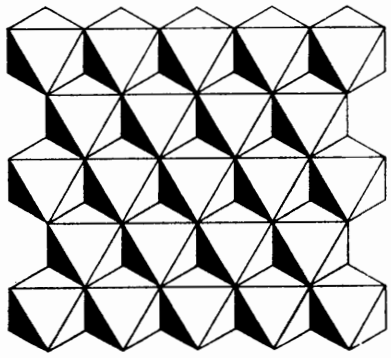

FIGURE 11 Anion vacancies of type C-M_2O_3 gathered on (111) plane

atoms and a shared plane of metal atoms adding $M_{1/2}O$ to give an overall composition $M_2\square O_3$. If this precursor is now sheared to eliminate the {111} plane of anion vacancies, the type A-M_2O_3 structure is obtained as is shown in Figure 12 (c). Elimination of the vacancies by a simple collapse along [111] of the precursor yields the energetically unfavourable situation of

contiguous metal–oxygen layer combinations of A_mA_o, B_mB_o, and C_mC_o. This is avoided by the c.s. $a/2\langle 100\rangle_{cub}$ restoring the cubic nature of the anion lattice and this, together with the corresponding co-operative shear movement of the metal lattice, gives the oxygen and metal-layer sequence characteristic of A-M_2O_3 shown in Figure 12 (c) [and Figure 7 (b)].

equilibria (*cf.* Table). Coherence at the various interfaces is illustrated in Figure 13. Hopefully, the intergrowth texture which must characterize the σ-region will eventually be revealed by high-resolution electron microscopy and lattice-imaging techniques.

It is apparent from the data in the Table that the composition x of the MO_x boundaries of the σ-phase

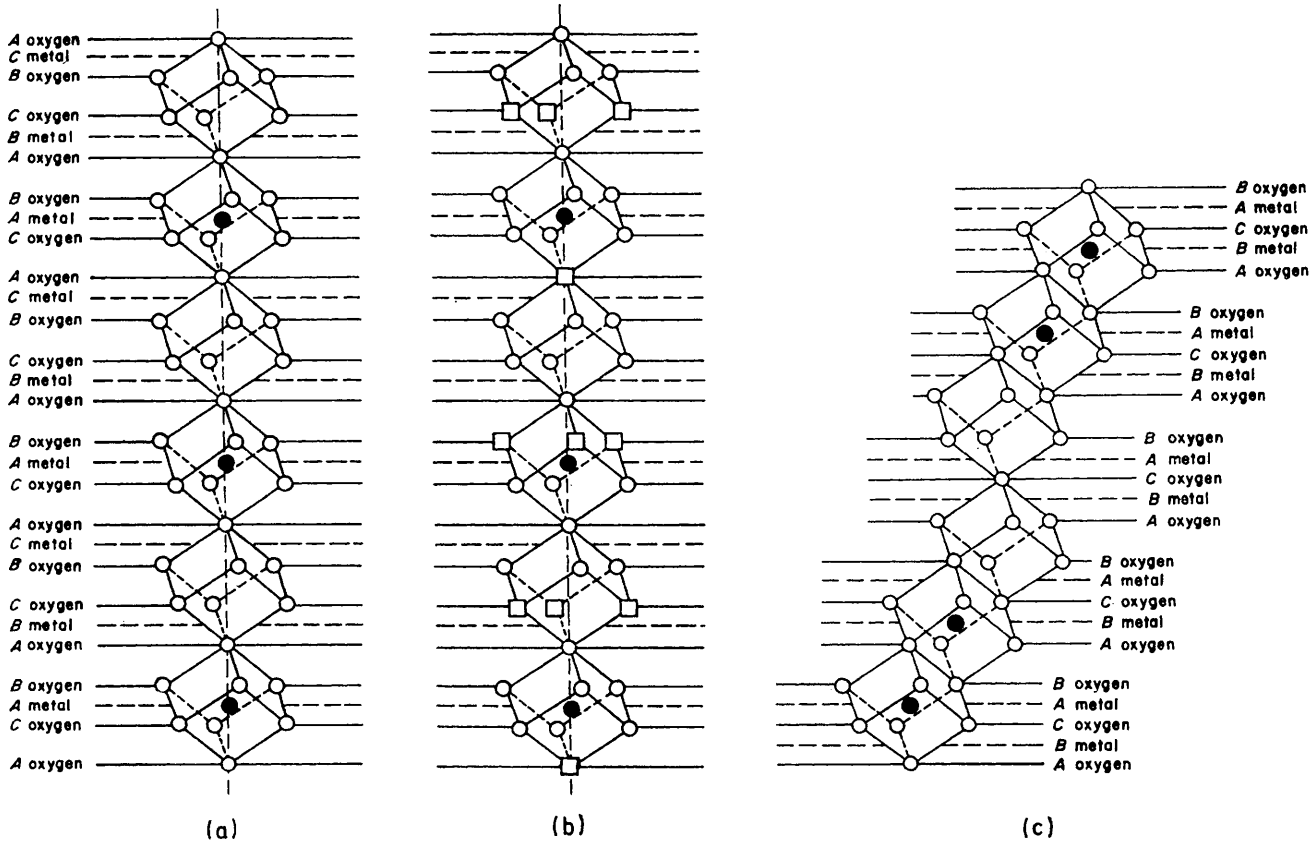

FIGURE 12 (a) The stacking sequence of metal and oxygen layers for $C1$-MO_2 in the vicinity of a three-fold rotation axis chosen to pass through atoms in the A layers of the cubic close-packed sequence. (b) Anion vacancies of type C-M_2O_3 assembled on every four (111) plane of precursor. (c) Type A-M_2O_3 structure formed by shearing precursor along vector $\frac{a}{2}[100]$

(IV) CONCLUSIONS

We conclude that the structural characteristics of the hyperstoicheiometric MO_x region can be illuminated by the formal procedure of systematically deleting (213) planes of composition $M_{1/2}O$ followed by c.s. of the parent ι-lattice. If the planes are removed in a regular manner, the sequence ι-M_7O_{12} ⟶ M_6O_{10} ⟶ M_5O_8 ⟶ M_4O_6 corresponding to the $n = 7$, 6, 5, and 4 members of the M_nO_{2n-2} homologous series is completed.

The extensive range of composition inhabited by the σ-phase (*e.g.* $1{\cdot}50 < x < 1{\cdot}72$ for M = Tb) is ascribed here to the intact cation lattice which remains essentially unchanged and the intrinsic coherence between the defect oxygen lattices of adjoining phases which comprise this region. Coherent intergrowth is expected at all compositions as the reduction of ι proceeds so that crystallization of the anticipated ordered homologues at $n = 5$ and 6 is inhibited, especially at the high temperatures required for establishment of the tensimetric

increases with oxygen pressure and temperature. This we ascribe to the rupture of the infinite linear chains of extended c.d.s which are corner-sharing in the σ_1-region, edge-sharing in the σ_2-region, and both corner- and edge-sharing in the σ_3-region. The smaller the chain length of the finite cluster, the larger the value of x in each of the σι-regions. The progression from order ⟶ disorder is attributed to the natural evolution from a regular deletion of $M_{1/2}O$ on (213) planes (which generates finite clusters of equal chain length) to an irregular omission which leads to finite clusters of varied chain lengths. However, coherence of the disordered phase is always preserved and continuity of the σ-phase is unaffected. For M = Pr, the limiting composition of the σ-phase approaches $PrO_{1.695}$. This corresponds to the rupture of corner-sharing chains in the σ_1-region into discrete dimeric clusters of composition $Pr_{13/2}\square_2O_{11}$ ($x = 1{\cdot}692$). Interestingly, the partial enthalpies and entropies in the oxidation branch of the

reaction $TbO_x + \delta/_2O_2 \longrightarrow TbO_{x+\delta}$ $(1{\cdot}5 \leqslant x \leqslant 1{\cdot}714)$ exhibit maxima [7] at the composition $TbO_{1{\cdot}69}$.

The origin of the miscibility gap $1{\cdot}695 < x < 1{\cdot}725$ for PrO_x-O_2 cannot be readily attributed to the nature of the defect oxygen lattice. If our proposed description of the region $1{\cdot}50 < x < 2{\cdot}00$ in terms of progressive

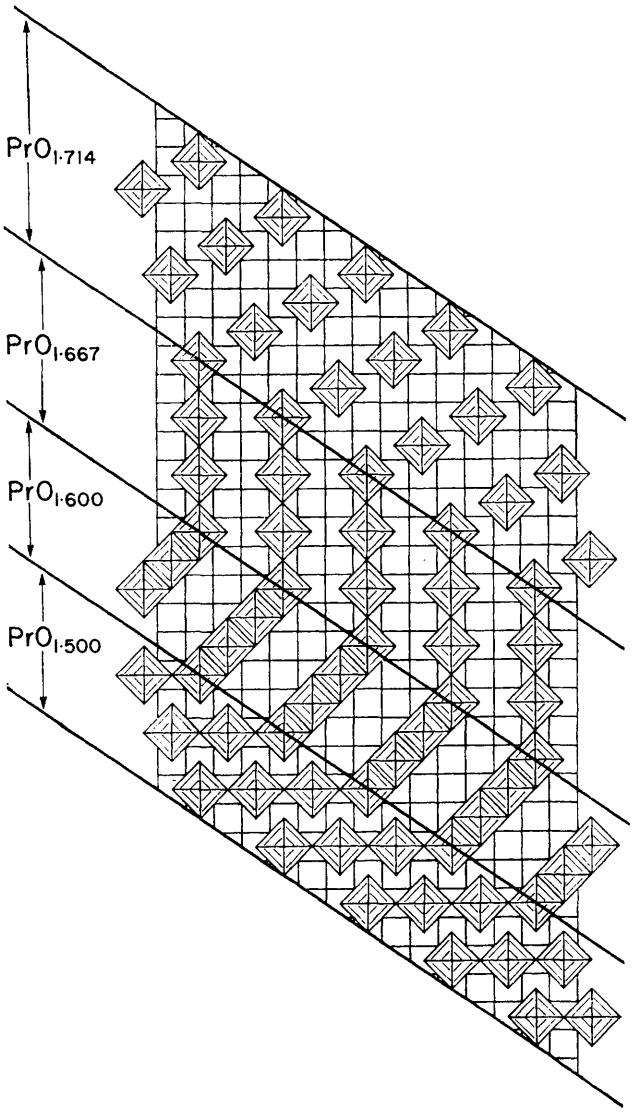

FIGURE 13 Coherence at various interfaces between ι-phase and reduced oxides in the σι-region

insertion or deletion of (213) planes of composition MO_2 is shown to be correct, then a miscibility gap at high temperatures would be unexpected for our idealized model. It seems more likely that immiscibility between the α- and σ-phases might arise from the basic mismatching between the b.c.c. and f.c.c. characteristics of the real σ- and α-metal lattices. Distortion of the metal lattice in the $D5_3$ compared with the $C1$ structure is substantial (of the order of 0·3 Å) and lack of coherence between σ- and α-phases is perhaps not surprising.

Hysteresis in oxidation–reduction pathways is a reflection of the close structural relationships which obtain in the σ-region. For example, it could be surmised that reduction of the rhombohedral ι-phase at higher temperatures might lead to infinite chains of σ-PrO_x in the univariant two-phase region [ι + σ]. Reoxidation of σ at slightly lower temperatures may then well result in rupturing of the chains into finite clusters of varied chain length so that the reoxidation branch [σ + ι]* will be characterized by different values of p, t, and x to generate a hysteresis cycle in the two-phase region. The (σι) pseudo-phase provides further phenomenological evidence for epitaxial continuity between the rhombohedral ι- and b.c.c. σ-phases in the hyperstoicheiometric region. The ι-phase will grow coherently as (σι) in oxidation (or shrink in reduction) at the expense of σ. It is not surprising that two phases are always detected by X-rays in the pseudo-phase region since the domains must possess linear dimensions of *ca.* 100—200 octants to give sharp diffraction lines.

The projection of the σ- and ι-phases into metastable regions of the phase diagram (σ^m and ι^m) at higher oxygen pressures and lower temperatures might likewise be ascribed to the close structural similarities which persist between the phases.

Comparison with Known Structures.—It is encouraging to note that, although no discrete homologues have been observed in the hyperstoicheiometric $MO_{1{\cdot}5+\delta}$ region for binary lanthanoid oxides, ternary phases of the composition $MO_{1{\cdot}667}$ are known. These include Cd_2UO_5 [41] and Sr_2UO_5.[41,42] The idealized structures of Cd_2UO_5 (X-ray [41]) and Sr_2UO_5 (neutrons [42]) are the same as the structure derived here by c.s. of ι-$M_{7/2}O_6$ [Figure 2 (c)]. Gorter [43] and Barker [44] have also obtained this structure by analysing the manner in which space-filling metal-centred polyhedra, for the co-ordination numbers 7(Cd^{2+}, Sr^{3+}) and 6(U^{4+}), can be packed to preserve a f.c.c. cation array.

The structure of β-Bi_2O_3 [45] also deserves brief comment because it represents a third way in which the stoicheiometry M_2O_3 can be achieved while preserving the identity of the $\square O_6$ co-ordination defect. Unlike the types C and D sesquioxide structures, octahedral co-ordination of anion vacancies is achieved by corner-sharing alone of c.d.s to yield an $\square O_3$ stoicheiometry. The $\square O_3$ network is reminiscent of the ReO_3 lattice, where the anion vacancies lie on Re sites, except that there are two interpenetrating ReO_3-like sub-lattices (*cf.* Figure 14). The relationship between this structure and type-D is extremely close, D being transformed into β-Bi_2O_3 by oxygen $\rightleftharpoons$ vacancy switches along every fourth [100] line of anion sites in each (010) layer [Figure 4 (a)] through a distance d. Clearly, there is a delicate balance in the energetics of the three M_2O_3

[41] M. Sterns and J. O. Sawyer, *J. Inorg. Nuclear Chem.*, 1964, **26**, 2291.
[42] B. P. Loopstra and H. M. Rietveld, *Acta Cryst.*, 1969, **B25(4)**. 787.
[43] E. W. Gorter, *J. Solid State Chem.*, 1970, **1**, 279.
[44] W. W. Barker, *Z. Krist.*, 1969, **128**, 55.
[45] G. Gattow and H. Schütze, *Z. anorg. Chem.*, 1964, **328**, 44.

structures based on the $C1$ lattice. It is significant that in all three, the structures adopted preserve octahedral co-ordination by oxygen of all the vacant anion sites and that the ensuing structures are determined uniquely by the topological requirements of the $\square O_6$ co-ordination polyhedron in the $C1$ parent matrix.

Finally, the recent single crystal studies [46] of β-$Pr_{12}O_{22}$ deserve comment. These have established a superstructure of monoclinic symmetry with unit cell dimensions of $a_m = 6{\cdot}6874$, $b_m = 11{\cdot}602$, $c_m = 15{\cdot}470$ Å, and $\beta = 120{\cdot}257°$. The volume of the unit cell is $48d^3$ and has been confirmed in electron diffraction studies.[10] Although the unit-cell volume is identical, we find that this monoclinic cell is not compatible with either the infinite rows of c.d.s along [$\bar{1}$20] or the [$\bar{1}\bar{1}$1] stacking arrangement proposed in Figure 8 (e) of Part I.[11] However, a structural model complying with these data can be derived if a discontinuity in the [$\bar{1}$20] rows of c.d.s and a modified-stacking principle are considered. There are four alternative directions along which a [$\bar{1}$20] chain of c.d.s might be branched ([210], [$\bar{2}$10], [$\bar{1}\bar{2}$0], and [$\bar{2}\bar{1}$0]) and it emerges that only one of these directions ([$\bar{2}$10]) permits a coherent structure compatible with the cell dimensions. Two possible $(001)_F$ layers, denoted A and B, derived from this principle are illustrated in Figure 15 (a), and it can be seen that in each a structural unit can be discerned with edge dimensions and directions bearing an identical relationship to the $C1$ fluorite structure as do the b_m and c_m axes of the monoclinic cell described above.[10] If these $(001)_F$ layers are then stacked in the sequence ABAB *etc.*, the unit cell for the resulting three-dimensional structure is identical to that given by Eyring *et al.*;[10] an $(1\bar{1}0)_F$ layer of this structure, showing the directions of the a_m and c_m axes, is illustrated in Figure 15 (b). It can be seen that the c.d.s are grouped in pairs, their centres separated by $a/2[111]$, so that the [$\bar{1}$20] and [$\bar{2}$10] rows of pairs constituting the structure may be regarded as fragments derived from (213) type

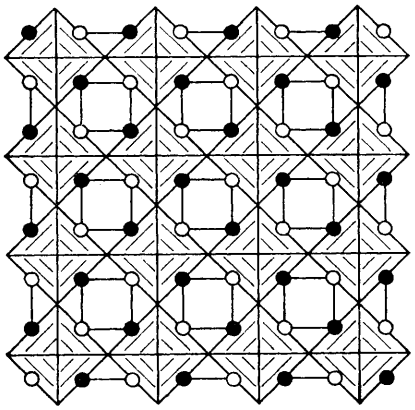

FIGURE 14 Arrangement of c.d.s in the reported [45] crystal structure of β-Bi_2O_3

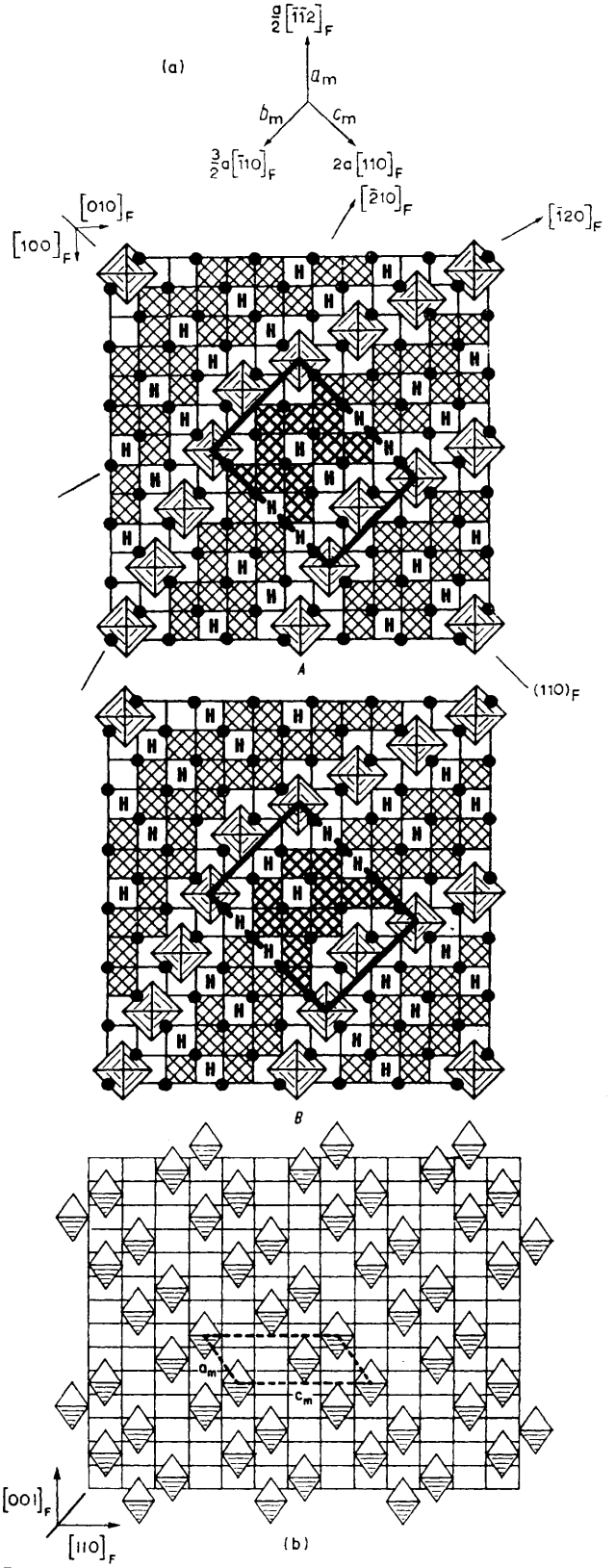

FIGURE 15 (a) Two $(001)_F$ layers, denoted *A* and *B*, containing a unit cell of the dimensions reported [46] for β-$Pr_{12}O_{22}$, showing the branching of [$\bar{1}$20] rows of c.d.s. The only difference between these layers is the location of the mating holes H. (b) An $(1\bar{1}0)_F$ layer of the structure proposed for β-$Pr_{12}O_{22}$, showing the chains of pairs of c.d.s arranged in the [$\bar{1}\bar{1}$2] direction. An outline of the monoclinic cell is shown

[46] M. Z. Lowenstein, L. Kihlborg, K. H. Lau, J. M. Haschke, and L. Eyring, Proc. 5th Materials Research Symposium, Nat. Bureau Standards Special Publ. No. 364, 1972, p. 343.

vacancy planes characteristic of ι-Pr_7O_{12}. The vacancy pairs are arranged in chains along the [$\bar{1}\bar{1}2$] direction [Figure 15 (b)]. This type of pairing,[47] a feature of the $Zr_{10}Sc_4O_{26}$ structure,[48] suggests a special role performed by the six-co-ordinated metal in coalescing the pairs having the composition $M_7O_{12}\square_2$. It is evident that the type of branching of [$\bar{1}20$] rows of c.d.s described here could be a source of crystal or chemical [49] twinning in this and other PrO_x phases.

We acknowledge stimulating discussions with Professor J. S. Anderson, F.R.S., and Professor D. J. M. Bevan.

[4/1376 *Received*, 8*th July*, 1974]

[47] J. O. Sawyer, B. G. Hyde, and L. Eyring, *Bull. Soc. chim. France*, 1965, 1190.

[48] M. R. Thornber, D. J. M. Bevan, and J. Graham, *Acta Cryst.*, 1968, **B24**, 1183.

[49] S. Andersson and B. G. Hyde, *J. Solid State Chem.*, 1974, **9**, 92.